European Journal of Pharmaceutics and Biopharmaceutics 126 (2018) 75–88

Contents lists available at ScienceDirect

European Journal of Pharmaceutics and Biopharmaceutics

journal homepage: www.elsevier.com/locate/ejpb

Research paper

A systematic reactor design approach for the synthesis of active pharmaceutical ingredients

Victor N. Emenike [a,b,c], René Schenkendorf [a,b], Ulrike Krewer [a,b,*]

[a] Institute of Energy and Process Systems Engineering, Technische Universität Braunschweig, Franz-Liszt-Straße 35, 38106 Braunschweig, Germany
[b] PVZ–Center of Pharmaceutical Engineering, Franz-Liszt-Straße 35A, 38106 Braunschweig, Germany
[c] International Max Planck Research School for Advanced Methods in Process and Systems Engineering, Sandtorstraße 1, 39106 Magdeburg, Germany

ARTICLE INFO

Article history:
Received 2 December 2016
Revised 8 March 2017
Accepted in revised form 15 May 2017
Available online 20 May 2017

Keywords:
Active pharmaceutical ingredients
Continuous pharmaceutical manufacturing
Intensified reactors
Optimization
Nucleophilic aromatic substitution
Elementary process functions

ABSTRACT

Today's highly competitive pharmaceutical industry is in dire need of an accelerated transition from the drug development phase to the drug production phase. At the heart of this transition are chemical reactors that facilitate the synthesis of active pharmaceutical ingredients (APIs) and whose design can affect subsequent processing steps. Inspired by this challenge, we present a model-based approach for systematic reactor design. The proposed concept is based on the elementary process functions (EPF) methodology to select an optimal reactor configuration from existing state-of-the-art reactor types or can possibly lead to the design of novel reactors. As a conceptual study, this work summarizes the essential steps in adapting the EPF approach to optimal reactor design problems in the field of API syntheses. Practically, the nucleophilic aromatic substitution of 2,4-difluoronitrobenzene was analyzed as a case study of pharmaceutical relevance. Here, a small-scale tubular coil reactor with controlled heating was identified as the optimal set-up reducing the residence time by 33% in comparison to literature values.

1. Introduction

Traditionally, batch processing is the standard in the fine chemicals and pharmaceutical industry because of its simplicity and flexibility [1]. However, batch manufacturing has some well-known disadvantages such as scale-up difficulties, mass and heat transfer bottlenecks, long production times and possible supply chain disruptions [2,3].

Continuous pharmaceutical manufacturing (CPM), in turn, is a process intensification strategy that enables the reduction of the number of synthesis steps and units, which can lead to significant cost savings [4,5]. Furthermore, CPM enables safer operation [3,6,7], better scalability, enhanced process automation, smaller process footprint, enhanced mass and heat transfer, and higher throughput [8]. As a result, CPM is considered by both academia and industry as the most viable alternative to batch manufacturing [9].

At the heart of the shift from batch to CPM technology are continuous flow reactors (or simply flow reactors), which are usually within the micro to millimeter scale. These reactors serve as the key driver of highly-intensified flow processes, and they can be intensified by using temperature, pressure, light or immobilization agents [10,11]. Hence, flow reactors are currently being used to synthesize APIs [12,13] and organic intermediates quite frequently [14]. Based on the advantages of flow reactors, Hessel proposed the concept of novel process windows (NPW), i.e. operating under extreme process conditions to improve API production [15].

However, Valera et al. [16] argued that the advantages cited for flow reactors might not always be the case and that the decision to operate a reaction continuously or batch-wise should be done on a case-by-case basis. Hence, the question arises: *how do we systematically choose the best reactor type for a particular API synthesis?*

In an attempt to answer this question, Plouffe et al. [17] proposed a tool box approach for the selection of the best reactor for a particular reaction based on reaction classes, reacting phase (single or multiphase), and the reaction network. However, the authors admitted that this heuristic-based approach might not encompass all reaction types [17]. Model-based approaches such as attainable region methods [18] and superstructure-reactor optimization [19] could be used, but these methods are still dependent on existing reactor types, i.e. following a component off-the-shelf philosophy.

Inspired by this challenge, we propose the use of an apparatus-independent methodology called elementary process functions (EPF) developed by Freund and Sundmacher [20,21]. A model-based approach such as the EPF methodology can guide the opti-

* Corresponding author at: Institute of Energy and Process Systems Engineering, Technische Universität Braunschweig, Franz-Liszt-Straße 35, 38106 Braunschweig, Germany.

E-mail address: u.krewer@tu-braunschweig.de (U. Krewer).

http://dx.doi.org/10.1016/j.ejpb.2017.05.007
0939-6411/

Nomenclature

Latin symbols

a	surface-to-volume ratio, mm^2/mm^3
C_i	molar concentration of component i, mol/L
$c_{p,i}$	specific heat capacity for component i, J/(mol K)
d_t	internal tube diameter (i.d.), mm
$E_{A,m}$	activation energy, J/mol
h	heat transfer coefficient, $kW/(m^2\ K)$
$\mathbf{j}$	component dosing flux vector, mol/min
j_q	heat flux i, $kJ/(s\ m^2)$
k_m	rate constant for reaction m, L/ (mol min)
$k_{\infty,m}$	pre-exponentional factor for reaction m, L/ (mol min)
K_e	environment fluid constant, m K/W
l	reactor length, m
Mwt	molecular weight, g/mol
N_{comp}	number of components, –
n_f	final amount of component i, mol
n_i	molar amount of component i, mol
$n_{i,0}$	initial amount of component i, mol
$n_{i,tot}$	total amount of moles of reactant i (2,4-difluoronitrobenzene or morpholine), mol
N_{reac}	number of reactions, –
r_m	rate of reaction m, mol/ (L min)
Re	Reynolds number, –
$\mathcal{S}$	selectivity, –
$\mathbf{s}^c$	selection vector (binary variable) for cases in level 1, –
t	reaction time of fluid element, min
T	reaction temperature, K
T_e	environment (cooling/heating) temperature, K
v	fluid velocity, mm/s
V	volume, mL
V_{EtOH}	volume of ethanol (solvent), mL
V_{reac}	volume of reacting components, mL
$\mathcal{X}$	conversion, –
z	axial coordinate, m
Bold font	vector-value variable

Greek symbols

$\nu_{i,m}$	stoichiometric ratio of component i in reaction m, –
γ	feed ratio of morpholine (**2**) to 2,4-difluoronitrobenzene (**1**), –
ΔH_m	standard ethalpy of reaction m, J/mol
μ_{EtOH}	viscosity of ethanol (solvent), cP [g/(s dm)]
ρ_{EtOH}	density of ethanol (solvent), g/dm^3
τ	residence time, min

Superscripts

c	cases considered in level 1

Subscripts

U	upper bound (or maximum allowable value)
L	lower bound (or minimum allowable value)
EtOH	ethanol (solvent)
reac	reaction or reacting components
i	component index
m	reaction index

mal design of intensified flow reactors and complement synthesis experiments. This can lead to novel process windows [15]; thereby, accelerating the pharmaceutical process development phase. As a case study of pharmaceutical relevance, we considered a homogeneous liquid phase nucleophilic aromatic substitution (S_NAr) of 2,4-difluoronitrobenzene in the presence of morpholine [22].

This paper is organized as follows: in Section 2, relevant approaches for designing reactors for API synthesis are reviewed. In Section 3, the EPF methodology is briefly described, and then demonstrated in Section 4 for the aforementioned case study. This is then followed by conclusions.

2. State-of-the-art on the design of reactors for APIs

In recent times, chemical reaction engineering (CRE) concepts are increasingly being applied to design reactors for the synthesis of APIs and organic intermediates [23–25]. For example, Shukla et al. [26] applied CRE principles to maximize the selectivity of a diazotization reaction in continuous flow reactors. Jolliffe and Gerogiorgis applied CRE and other process engineering tools to design a conceptual process for the continuous manufacturing of ibuprofen [25] and artemisinin [27]. By applying CRE tools, Nagy *et al.* [23] derived simple heuristics for determining when it is important to consider dispersion or mixing in flow reactor design, dimensioning, and scale-up. Witt *et al.* [24] compared models of varying complexity for the design of mesoscale flow reactors. Westermann and Mleczko [28] applied CRE principles to highlight the importance of considering heat management (which is usually ignored) in the design of continuous flow reactors for organic synthesis. However, the aforementioned studies are based on the selection of "off-the-shelf" reactors; thus, limiting the possibility of novel reactors or the selection of the best existing reactor.

Moreover, chemical engineers and chemists in pharmaceutical drug development rely on established types of flow reactor during their modeling and simulation or laboratory protocols. As described by Roberge [17,29], there are three basic flow reactors used in API synthesis, namely: plug flow (coil) reactors, continuous-stirred tank reactors (CSTRs), and plate reactors. Furthermore, new types of reactors such as the multi-injector reactor [30,31], the continuous oscillatory baffled reactor [32], the agitated cell reactor [33], and the filter reactor [34] have been developed and applied to CPM. Experimentally, it is almost impossible to compare all possible candidates of flow reactors for a particular synthesis protocol due to cost and time constraints. Even for a small subset of available reactors at the lab scale, it is infeasible to consider all possible reactor configurations in the design space and to determine the underlying optimal operating conditions by means of experimental trial-and-error.

Furthermore, most of the continuous flow reactor modeling activities reported in the current literature are based on simulations with little or no model-based optimization studies. Even though a number of optimization-based reactor design approaches exist [19,18], these methods still depend on established reactor types. Therefore, the possibilities for the optimal design of new intensified reactors are limited. Here, an apparatus-independent concept such as the elementary process functions (EPF) might be an interesting alternative. In this work, the focus is on demonstrating how the EPF approach can be used to design optimal reactor configurations for API synthesis problems.

3. Elementary process functions-based reactor design

The elementary process functions (EPF) methodology proposed by Freund and Sundmacher [20] was used in this work for a sys-

tematic optimal reactor design in the field of API synthesis. The EPF approach breaks-free from the conventional unit-operation approach which is usually based on "off-the-shelf" processing units such as mixers, reactors, distillation columns, etc. The key idea is to replace units with functional modules and track a fluid element traveling through these functional modules. In each functional module, e.g. a reaction module, the changes of the state of a fluid element with time are influenced by fluxes (controls) such as heat fluxes, component dosing fluxes, and diffusion fluxes (see Fig. 1).

Based on the EPF approach, Peschel et al. [21] developed a systematic reactor design methodology. Here, the optimal reaction route in state space with respect to a particular objective function is obtained. Examples of these objective functions include minimal residence time, highest possible conversion or selectivity. As a result, various process intensification methods can be incorporated into the reactor design process. In literature, it has been shown that this concept can lead to novel intensified optimal reactors [21,35,36]. In the sequel, we briefly explain the three levels of the EPF-based reactor design approach: (i) integration and enhancement, (ii) control variable selection, and (iii) technical approximation. For a more detailed discussion, the reader is referred to [21] and references therein.

3.1. Level 1: Integration and enhancement

On the first level, process intensification concepts [37] such as integration and enhancement are considered. Here, integration refers to a unit with more than one function e.g. reactive distillation column; while enhancement involves the use of fluxes such as heat flux and component dosing fluxes to improve the process. Typically, the intensification concepts are chosen based on the reactor designer's experience, but a more systematic approach such as the superstructure optimization concept [19] might be implemented as well at this stage. Furthermore, the optimal reaction route is obtained under the influence of fluxes optimized along the path of the fluid element, and no limitations arising from predefined reactors are imposed. The only constraints are due to thermodynamic relations, reaction kinetic, and system-inherent features such as temperature bounds and solubility.

The dynamic behavior of the representative fluid element is modeled by the Lagrangian approach [38] to incorporate the non-geometric and apparatus-independent nature of EPF. Moreover, this formulation leads to short computation times and relatively fast screening of various process intensification (PI) options with the purpose of identifying an optimal reaction route [21]. Ultimately, the goal of the first level is to determine the best theoretically possible reaction route which will serve as a benchmark for the next two levels and any final reactor implementation.

3.2. Level 2: Control variable selection

At the second level, technically implementable control variables are selected to approximate the pre-defined flux profiles from level 1. This is because heat flux and component dosing fluxes can be limited by heat transfer kinetics and mass transfer kinetics in reality.

Furthermore, the flow regime, a particular channel geometry, and a prototype reactor set-up are assumed at this level. Finally, the best control variables that lead to an optimal objective value close to that of the first level are selected, and realized in the third level.

3.3. Level 3: Technical approximation

The technical approximation can be achieved by using off-the-shelf reactors or by novel design principles based on the optimal reaction route and related control profiles from the previous levels. Nevertheless, it should be mentioned that the technical approximation of the reaction route and control profiles are not unique but are dependent on the engineering judgement of the reactor designer.

It is also possible to consider different hypothetical technical reactors within a superstructure framework [19] comparing various configurations simultaneously. As soon as a suitable reactor design is chosen, simple and rigorous reactor models can be formulated and optimized in order to ascertain the optimally fine-tuned configuration of the identified reactor. Lastly, the three levels led to a class of mathematical problems called dynamic optimization problems. The details of the solution approach used to solve them can be found in Section 3.4.

3.4. Dynamic optimization solution strategy

The EPF approach is expressed mathematically as a dynamic optimization problem which has to be solved efficiently. In this work, a direct ("discretize-then-optimize") solution approach was used. For each level considered in this work, the dynamic mole balances, energy balances, constitutive equations, and algebraic constraints constitute a system of differential algebraic equations (DAEs).

These DAEs were transcribed into a large scale system of nonlinear equations by using the simultaneous dynamic optimization solution approach [39]. The simultaneous approach was selected because it handles instabilities and path constraints efficiently [39,40]. Specifically, the DAEs were transcribed by using the method of orthogonal collocation on finite elements [41]. The resulting system of nonlinear equations was implemented in the algebraic mathematical language AMPL [42] by using the CONOPT solver [43]. All computations were performed on a PC running a CentOS operating system with an Intel(R) Core(TM) i7-4789 processor at 3.60 GHz, and 16 GB RAM.

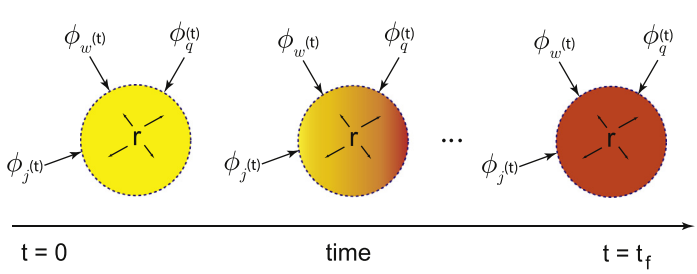

Fig. 1. Conceptual representation of a fluid element in thermodynamic state space affected by generic time-varying component dosing fluxes $\phi_j(t)$ and $\phi_w(t)$, the reaction flux r, and heat flux $\phi_q(t)$.

4. Optimal reactor design for the nucleophilic aromatic substitution of 2,4-difluoronitrobenzene

We applied the EPF approach for an optimal reactor design of the nucleophilic aromatic substitution (S_NAr) of 2,4-difluoronitrobenzene. This model reaction was chosen because of its pervasive utility in the pharmaceutical industry [44–46] and the availability of kinetic data [22]. The related reaction kinetics and mechanism used in this work was adapted from the work by Lee et al. [22] (see Fig. 2). According to this reference, it was assumed that species in charged ionic form are negligible. O'Brien and co-workers also reported that the salt byproduct **6** was removed by an extraction process [44]. Hence, **6** would not be considered in the reaction mechanism as shown in Fig. 3. Furthermore, hydrogen fluoride (HF) is assumed not to be in the gaseous form as it can form ionic bonds with the amine groups of the reaction products and reactant **2** [22]. HF can also form alcohol–HF mixtures with the ethanol solvent as stated in Ref. [47]. However, these were not considered in this study in order to keep the model complexity tractable. These assumptions are also supported with the fact that the reactions were handled in the homogeneous liquid phase by Lee *et al.* [22]. The objective of this work is to design an optimal reactor that minimizes the residence time of the S_NAr reaction between 2,4-difluoronitrobenzene (**1**) and morpholine (**2**). The corresponding decision structure for the reactor design procedure is shown in Fig. 4 and explained in more detail in the sequel.

4.1. Level 1: Applying integration and enhancement concepts

In this work, three process-intensifying cases (see Fig. 4) were be considered with the objective to minimize the residence time of the studied reaction system. These include:

1. Reactor intensification by heat-flux/reaction temperature optimization as a generic concept for minimizing the residence time [48].
2. For the remaining two cases, we consider the concept of component flux dosing. This intensification method was chosen because dosing strategies may lead to reduced residence times while leading to better temperature control and mitigation of hot spots [31,49].

For the sake of comparison, the proposed options are benchmarked against an optimal reference case from literature [22]. Here, an isothermal tubular (coiled) flow reactor was optimized by simulation and experimental studies. The optimal residence time, temperature, feed-ratio of morpholine (**2**)-to-2,4-difluoronitrobenzene (**1**), and selectivity were 5 min, 393.15 K, 2.7, and 87%, respectively. Next, we explain each intensification and enhancement concept considered in more detail.

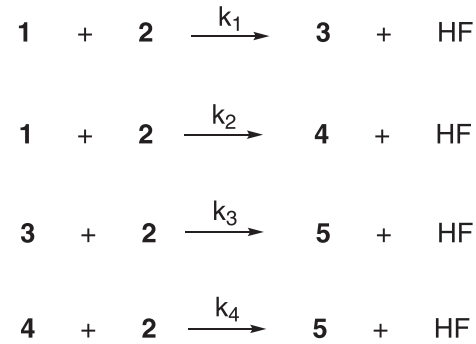

Fig. 3. Reaction mechanism for the nucleophilic aromatic substitution of 2,4-difluoronitrobenzene.

Case 1. Fluid element without dosing.

In this case, the feed ratio and heat flux are optimized assuming ideal unconstrained fluxes (on the first level). Technically, we mimic heat flux changes by using the reactor temperature as the control variable while the feed ratio will be an additional design parameter.

Case 2. Fluid element with dosing of **1**.

Case 2 is similar to case 1, with the addition of another control variable: the component dosing flux of reactant **1** along the reaction route. This enables us to consider the possibility of an enhancement concept that involves the interplay between the optimal heat flux and reactant **1** dosing profiles.

Case 3. Fluid element with dosing of **2**.

Case 3 follows the same idea as case 2, but with reactant **2** dosed along the reaction coordinate instead of reactant **1**. This strategy enables us to consider the effect that the optimal heat flux and reactant **2** dosing will have on the residence time.

4.1.1. Model development for the EPF level 1

The mole balances are formulated by using the Lagrangian approach. Furthermore, the reaction was assumed to be carried out entirely in the liquid phase, and the solvent volume was assumed to be equal to or larger than the volume of reacting species. Thus, the densities of each component and the volume of the fluid element were assumed to be constant. We assume constant concentration for the solvent, ethanol, while the mole balances for the other reaction components i (see Fig. 2) are given as:

$$\frac{dn_i(t)}{dt} = \mathbf{s}^{c^\top} \cdot \mathbf{j}(t) + \sum_{m}^{N_{reac}} \nu_{i,m} \cdot r_m \cdot V \quad \forall i \in \{\mathbf{1}, \mathbf{2}\}, \tag{1}$$

$$\frac{dn_i(t)}{dt} = \sum_{j}^{N_{reac}} \nu_{i,m} \cdot r_m \cdot V \quad \forall i \in \{\mathbf{3}, \mathbf{4}, \mathbf{5}, \mathrm{HF}\}, \tag{2}$$

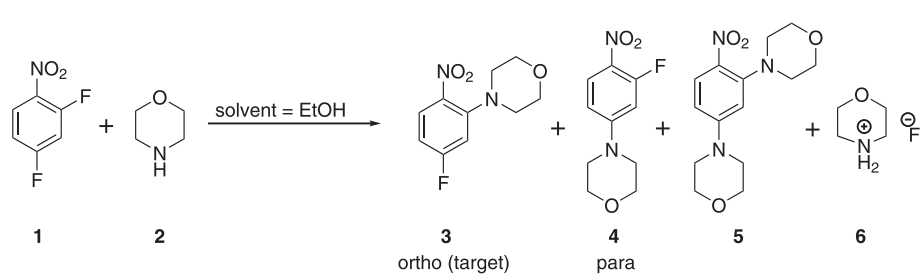

Fig. 2. Reaction scheme for the nucleophilic aromatic substitution of 2,4-difluoronitrobenzene (**1**) with morpholine (**2**) to produce the ortho regio-selective isomer **3**, para regio-selective isomer **4** and by-products **5** and **6**.

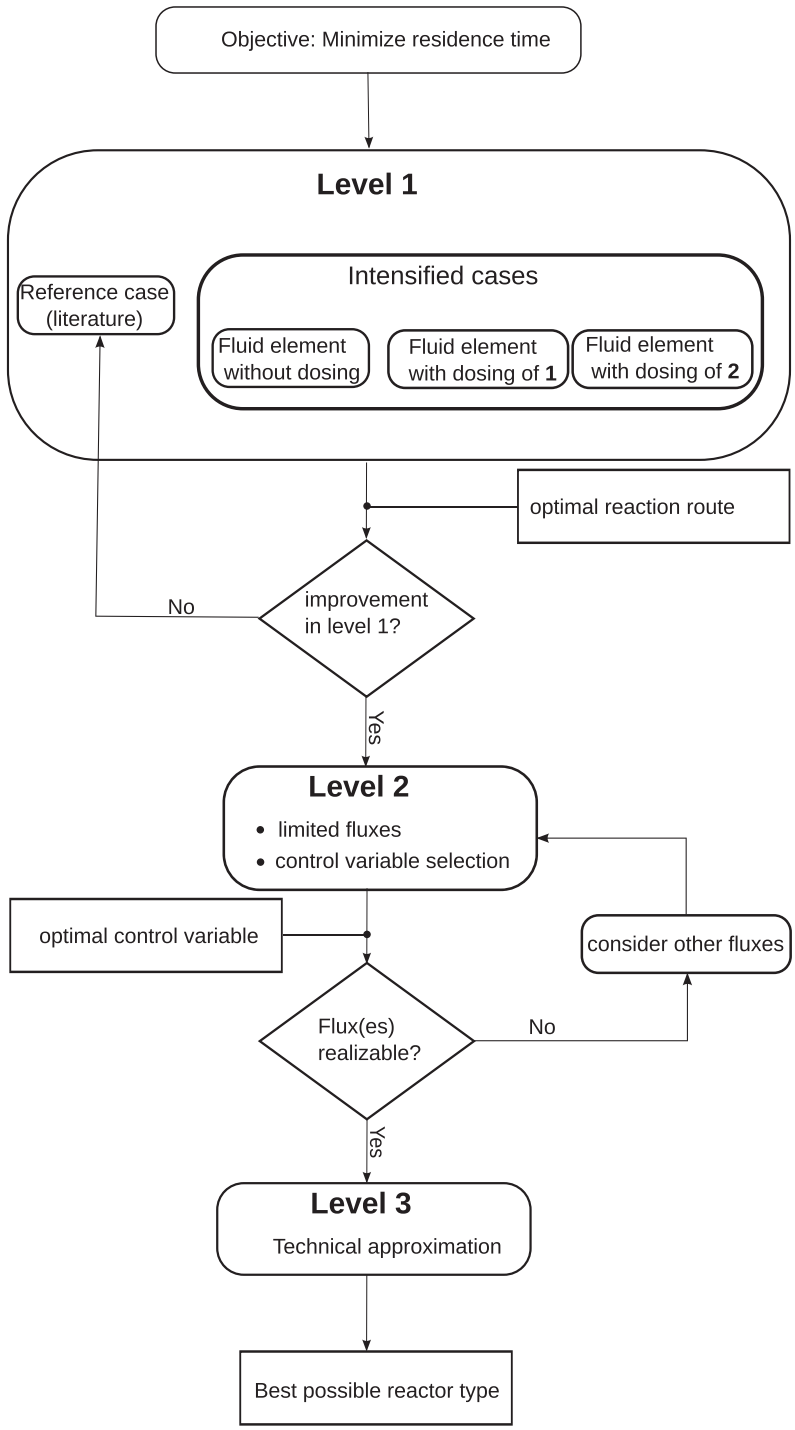

Fig. 4. EPF decision structure for the intensified reactor design.

where $\mathbf{j}(t) := [j_1(t), j_2(t)]^\top$ is a vector representing the component dosing fluxes with $j_1(t)$ and $j_2(t)$ representing dosing of **1** and **2**, respectively. $\mathbf{s}^c$ is a selection vector which determines the dosing fluxes are considered in each case $c \in \{1,2,3\}$. $\mathbf{s}^c$ is set as [0,0], [1] and [0,1] for cases 1, 2, and 3, respectively. $\nu_{i,m}$ is a stoichiometric ratio of component i in reaction m, r_m is the rate of reaction m and V is the volume of the fluid element. Typically, the volume is formulated as a function of the number of moles, temperature dependent density, and molecular weight of the reaction species [50]. However, with the unavailability of temperature dependent density equations for the S_NAr reaction molecules, we have assumed a constant volume of 10 mL [22] in this study. This assumption is plausible since we do not expect significant volume changes in small scale systems with a single organic phase. Furthermore, the stoichiometric ratios $\nu_{i,m}$ follow the reactions in Fig. 3. The reaction rates r_m are expressed by power law kinetics as postulated by Lee et al. [22] according to:

$$r_m = k_m \prod_i^{N_{\text{comp}}} C_i^{|\nu_{i,m}|} \quad \forall m \in N_{\text{reac}} \tag{3}$$

where N_{comp} is the number of reacting components, N_{reac} is the number of reactions and the rate constants k_m for each reaction m is given by the Arrehenius equation:

$$k_m = k_{\infty,m} exp\left(\frac{-E_{A,m}}{RT}\right) \tag{4}$$

where $k_{\infty,m}$ and $E_{A,m}$ are the pre-exponential factor and activation energy for reaction m, respectively. The values for $k_{\infty,m}$ and $E_{A,m}$ were taken from [22] and are given in Table 1.

Lastly, performance measures such as conversion $\mathcal{X}$ and selectivity $\mathcal{S}$ are presented below:

$$\mathcal{X} = \frac{n_{\mathbf{1},\text{tot}} - n_{\mathbf{1},0}}{n_{\mathbf{1},\text{tot}}} \tag{5}$$

$$\mathcal{S} = \frac{n_{\mathbf{3},f} - n_{\mathbf{3},0}}{\mathcal{X} \cdot n_{\mathbf{1},\text{tot}}} \tag{6}$$

where $n_{\mathbf{1},tot}$ is the sum of the initial amount and dosed amount of 2,4-difluoronitrobenzene, and $n_{\mathbf{3},f}$ is the final amount of the target product at the end of the reaction.

4.1.2. Optimization formulations for level 1

A case-dependent dynamic optimization formulation for minimizing the residence time τ is described as:

$$\min_{T(t),\mathbf{s}^\top \mathbf{j}(t),n_{\mathbf{1},0},\gamma} \tau$$

subject to:

- Mole balances: Eqs. (1) and (2)
- Reaction rates: Eqs. (3) and (4)
- Performance measures: Eqs. (5) and (6)
- Terminal constraints: $\mathcal{X} = 0.99$
- Intrinsic bounds: $T \in [T_L, T_U], \gamma \in [\gamma_L, \gamma_U]$
- System bounds: $\mathcal{S} \in [0,1], n_{\mathbf{i},\text{tot}} = n_{\mathbf{i},0} + \int_0^\tau j_i dt \ \forall i \in \{\mathbf{1},\mathbf{2}\}$
- Case specific selection vector: $\mathbf{s}^c$

In addition to the residence time, other objective functions such as the yield maximization [21], selectivity maximization [36], space time yield maximization [51] or even multi-objective functions can be evaluated depending on the problem at hand. In this work, the conversion was set at 99% to avoid challenges in downstream separation [22]. As conversion is nearly complete ($\mathcal{X} = 0.99$) and is set as a terminal constraint, it is not expedient to use the final conversion as an objective function. Furthermore, we conducted preliminary studies using the selectivity as the objective function and found that the selectivity and yield cannot be improved as explained in the next section. Therefore, the residence time was selected as the objective function for this study.

The temperature range, 353.15–393.15 K at which the kinetic experiments were performed were used to define the lower bound T_L and upper bound T_U on the temperature control variable. Similarly, the upper and lower bounds of the feed-ratio γ of reactant **2** to **1** were chosen as $\gamma_L = 1$ and $\gamma_U = 3$, respectively. This was done in order to ensure that the reaction kinetics remain valid throughout the optimization procedure. Please note, to ensure a fair comparison with the literature reference case, these constraints are applied here as well.

Table 1
Reaction kinetic parameters taken from Lee et al. [22].

Reaction	k_∞ [L/(mol min)]	E_A [J/mol]
r_1	1.8673×10^6	43.6×10^3
r_2	1.7514×10^4	35.8×10^3
r_3	9.7012×10^3	40.4×10^3
r_4	6.1063×10^8	70.1×10^3

4.1.3. Results for EPF level 1

The dynamic optimization result of the first case in level 1 is shown in Fig. 5. The concentration profiles and temperature control profile are shown in Fig. 5a and b, respectively. The residence time for the first case (i.e. no dosing) in level 1 is 3.22 min which is a 35% decrease from the reference case [22] that was optimized by combining experiments and simulations. It can be seen in Fig. 5b that the temperature profile remains at the upper bound of 393.15 K. This is due to the fact that the reaction would ideally be completed in the shortest possible time if it operates at the highest possible temperature throughout the course of the reaction. The temperature profiles of the second and third cases (i.e. dosing of **1** and **2**) are equal to that of the first case and thus not shown here. Nevertheless, the temperature profile implies that operating at the maximum temperature leads to the shortest residence time. Also, the ratio of reactant **2** to reactant **1** for the case 1 is 3 to 1, i.e. the upper bound.

The intensification strategies at level 1 show that the dosing of reactants does not lead to lower residence times or higher selectiv-

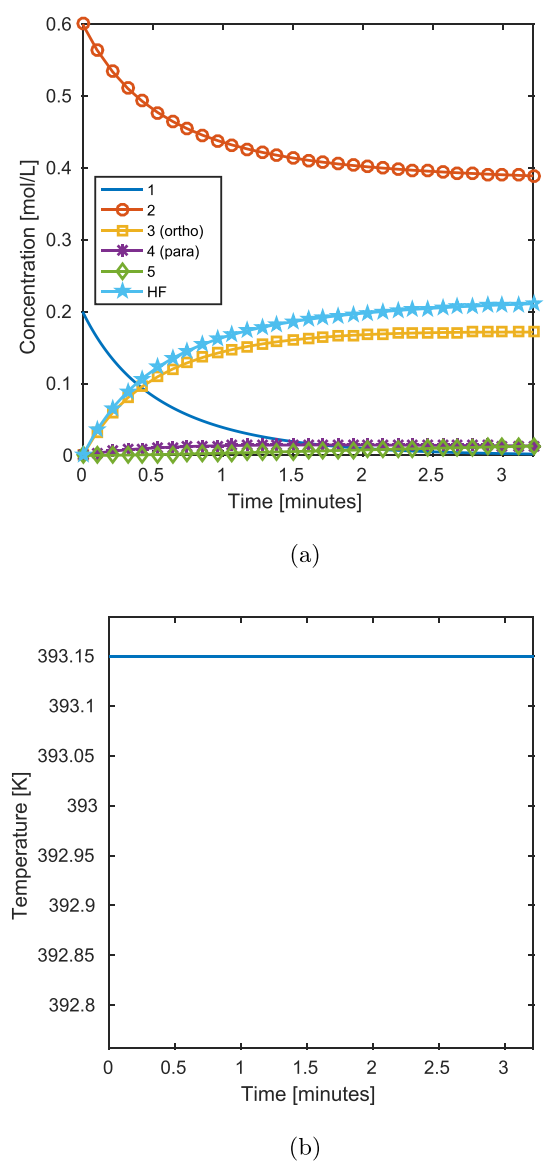

Fig. 5. Optimization results for the first level in the case of the fluid element without dosing (τ = 3.22 min, γ = 3.00): (a) concentration state profiles; (b) temperature control profile.

ity (see Appendix A and Figs. A.13 and A.14). This is due to the fact that the reaction order of reactants **1** and **2** are the same in the desired and undesired reactions. Hence, the dependence of reaction rates on the concentration of reactants **1** and **2** in the desired and undesired reactions are the same.

Moreover, the reactions are all irreversible and purely driven by the kinetics and not by thermodynamics. This kind of reaction is termed neutral as reported in Lu et al. [52] and Hamel *et al.* [53]. Therefore, the only way to minimize the residence time is to exploit the heat flux and feed ratio of reactants **1** and **2**.

In the next section, we seek to implement the idealized heat flux obtained by incorporating an energy balance that includes transport kinetics to obtain realistic heat fluxes.

4.2. Level 2: Limited fluxes and control variable selection

In level 2, the major goal is to select physically implementable control variables that can approximate the control profiles obtained in level 1. In detail, we have to add transport kinetic limitations on the heat flux in terms of material and environmental factors.

4.2.1. Model development for level 2

In addition to the model equations in level 1, an energy balance is included as shown below:

$$\left(\frac{\sum_i^{N_{\text{comp}}} n_i c_{\text{p},i}}{V_{\text{reac}}} + \frac{\rho_{\text{EtOH}} \cdot c_{\text{p,EtOH}}}{\text{Mwt}_{\text{EtOH}}}\right)\frac{dT}{dt} = -\left(a \cdot j_{\text{q}} + \sum_m^{N_{\text{reac}}} r_m \cdot \Delta H_m\right) \tag{7}$$

where $c_{\text{p},i}$ is the specific heat capacity of component i in J/(mol K) which is expressed as temperature dependent equation (see Appendix C). V_{reac} is the total volume of the reacting species (excluding the solvent) in L, and ρ_{EtOH} is the density of the solvent (ethanol) in g/L. Mwt_{EtOH} is the molecular weight of ethanol in g/mol, $a(= 4/d_{\text{t}})$ is the surface-to-volume ratio in mm^2/mm^3, and j_{q} is the heat flux in J/(s m^2). The standard enthalpies of reactions ΔH_m were taken from Ref. [22]. The heat flux j_{q} transport kinetics is assumed to follow Fourier's law and it is given as:

$$j_{\text{q}} = h(T - T_{\text{e}}) \tag{8}$$

where h is the heat transfer coefficient which is kept at a constant value of 0.5 kW/(m^2 K) [36], and T_{e} is the environment (heating or cooling) temperature in Kelvin (K). For more details on the model formulation of the energy balance for level 2, the reader is referred to Appendix B.

4.2.2. Optimization formulations for EPF level 2

The optimization formulation of level 2 has the same structure as that of level 1, but with changes in the state and control vectors, and with additional variables and constraints. Since an energy balance is on the second level, the reaction temperature is now considered as a state variable and not as a control variable.

Moreover, the volume of the solvent V_{EtOH} is chosen as a decision variable within reasonable bounds and the volume of the reacting species V_{reac} is constrained by the equality constraint:

$$V_{\text{reac}} = V - V_{\text{EtOH}} \tag{9}$$

Furthermore, a soft constraint was included to minimize the heat loss by limiting the difference between the initial temperature T_0 and final temperature T_f to a maximum of 1 K:

$$(T_f - T_0)^2 \leqslant 1 \tag{10}$$

Due to the small volume of the reactor considered in this work, the corresponding bound on the tube diameter was set between 1 and 1.5 mm [10,54]. Therefore, the optimization of the second level is given as follows:

$$\min_{\{T_{\text{e}}(t), d_{\text{t}}, V_{\text{EtOH}}, n_{\mathbf{1},0}, \gamma\}} \tau$$

subject to:

- Mole balances: Eqs. (1) and (2)
- Energy balance: Eq. (7)
- Heat flux transport kinetics: Eq. (8)
- Reaction rates: Eqs. (3) and (4)
- Performance measures: Eqs. (5) and (6)
- Volume constraint: Eq. (9)
- Terminal constraint: $\mathcal{X} = 0.99$
- Heat loss constraint: Eq. (10)
- Intrinsic bounds: $T \in [T_{\text{L}}, T_{\text{U}}], T_{\text{e}} \in [T_{\text{eL}}, T_{\text{eU}}], \gamma \in [\gamma_{\text{L}}, \gamma_{\text{U}}]$
- Design bounds: $d_{\text{t}} \in [d_{\text{tL}}, d_{\text{tU}}]$
- System bounds: $\mathcal{S} \in [0, 1]$

The bounds of the reaction temperature are similar to those of level 1, while the environment temperature T_{e} is set to reasonable bounds from 300 to 393.15 K. The parameters and bounds used in the optimization formulation for level 2 are summarized in Table 2.

4.2.3. Results for level 2

In the case of limited kinetics, the minimum residence time and selectivity for the reaction are approximately 3.31 min and 87%, respectively. This slight increase in residence time of about 2.9% is due to Eq. (10) and the non-idealities incorporated in level 2. Obviously, the environment temperature is a suitable control variable for implementing the reaction route and corresponding control profiles. Furthermore, the optimal solvent volume, tube diameter and the feed ratio obtained are 5 mL, 1 mm and 3.0, respectively.

The concentration profiles are nearly identical to those of case 1 in level 1 (cf. Fig. 5) while the heat flux and temperature profiles are shown in Figs. 6 and 7, respectively. The temperature profile rises from the initial temperature of 353.15 K to the upper bound, 393.15 K within the first 15 s and remains at the upper bound for approximately 3 min until the 99% conversion condition is fulfilled. Subsequently, the temperature decreases to 354.15 K in the shortest possible time in order to fulfill the heat loss constraint (Eq. (10)). The heat flux profile shows the initial heating of the reaction fluid to its maximum allowable temperature, followed by a zero heat flux due to no temperature gradient between the reaction temperature and environment temperature, and then cooling in the last step. This temperature profile was caused by the environment temperature which remains at its highest value of 393.15 K for the first 3.21 min before switching to its lower bound of 353.15 K (cf. Fig. 8).

As seen, the temperature has a strong impact on the residence time. Therefore, to quantify additional factors a sensitivity study was applied as shown below.

Table 2
Optimization parameter values used in level 2.

Parameters	Values	Units
h	0.5	kW/(m^2 K)
T_0	353.15	K
T_{L}	353.15	K
T_{U}	393.15	K
T_{eL}	353.15	K
T_{eU}	393.15	K
γ_{L}	1	–
γ_{U}	3	–
d_{tL}	1	mm
d_{tU}	1.5	mm

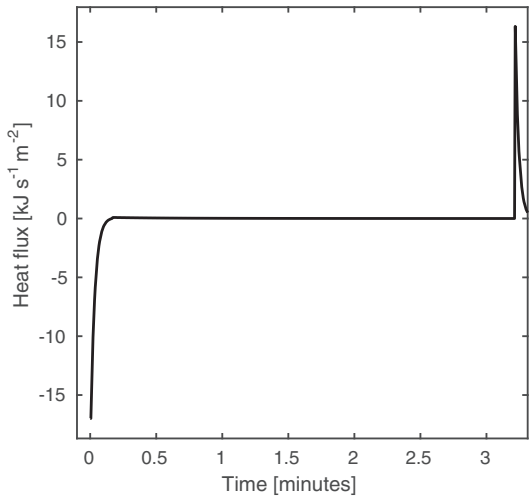

Fig. 6. Heat flux profile for EPF level 2.

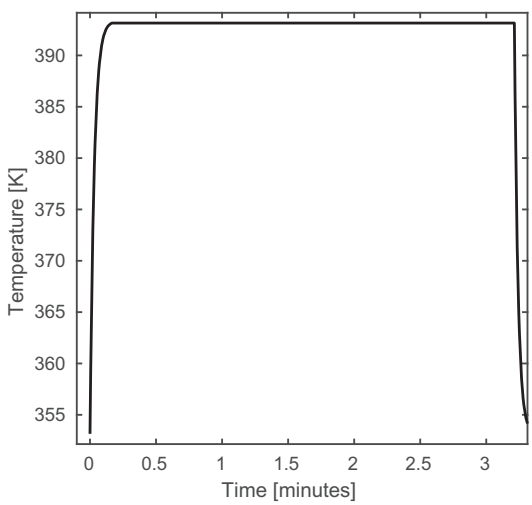

Fig. 7. Temperature state profile for EPF level 2.

4.2.4. Parameter sensitivity analysis

In this section, a sensitivity analysis on the selected case in level 2 is performed in order to determine the effect of certain design parameters before moving on to the technical approximation. The heat transfer coefficient and tube diameter were selected as two parameters of interest. Typically, these two parameters determine the cost of the resulting technical reactor. Another important reason for a sensitivity study is to ensure that the aforementioned parameter ranges and assumed values in level 2 do not affect the model and objective adversely.

Firstly, a parameter sensitivity analysis was performed by varying the heat transfer coefficient, h between 0.5 and 5 kW/(m^2 K) as reported by Kockmann et al. [54], while the diameter was kept at the constant optimal value of 1.0 mm. For a selected value of h within this interval (see Fig. 9a), an optimization problem was solved to determine the corresponding residence time and selectivity. Fig. 9a shows that increasing the heat transfer coefficient reduces the residence time, and that the selectivity remains at a constant value of approximately 86.4% over the whole range. Moreover, the residence time between 3 and 5 kW/(m^2 K) remains at a constant value of 3.25 min and does not reach the 3.22 min attained in level 1. This is because of the additional constraint Eq. (10) and the fixed initial temperature of 353.15 K on level 2.

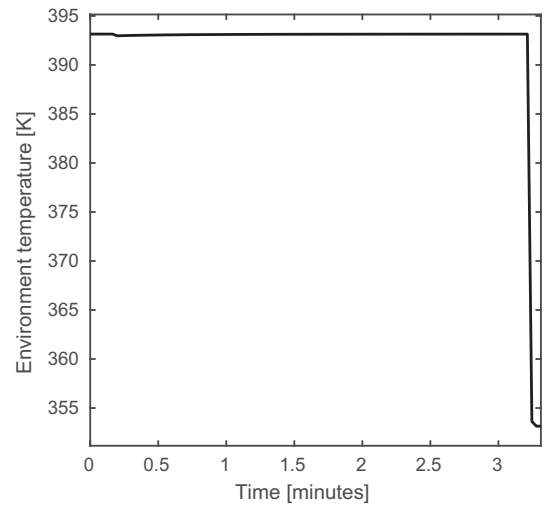

Fig. 8. Environment temperature control profile for EPF level 2.

Another reason is that the reaction temperature is a state variable and not a control variable in level 2.

In addition, a parameter sensitivity analysis was performed by varying the internal tube diameter, d_t between 0.1 and 2 mm [54,22], while the heat transfer coefficient was kept at the constant

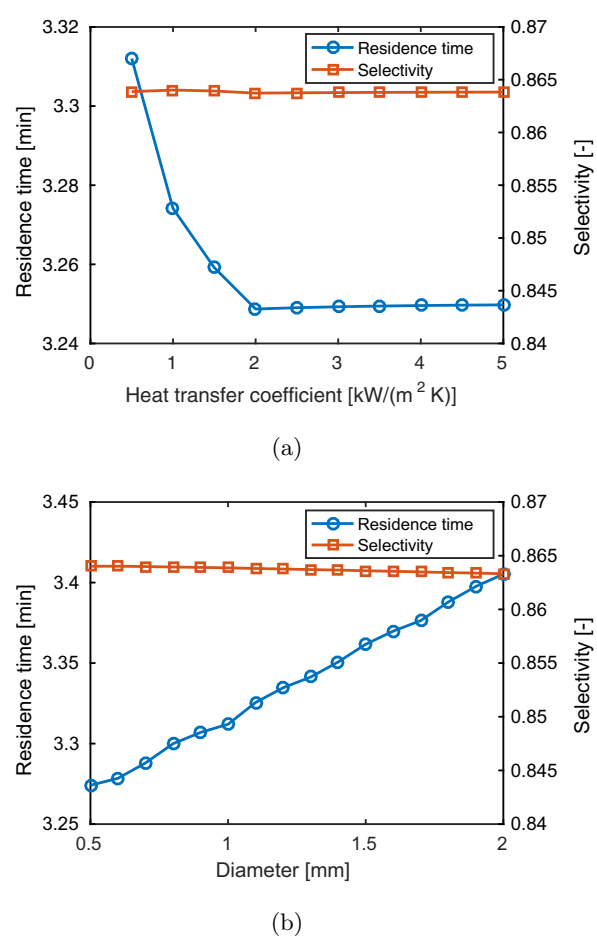

Fig. 9. Sensitivity analysis for the environment temperature control case in EPF level 2: (a) effect of heat transfer coefficient on residence time and selectivity; (b) effect of tube diameter on residence time and selectivity.

previously assumed value of 0.5 kW/(m^2 K). Similar to the sensitivity analysis for the heat transfer coefficient, optimization problems were solved at selected values of d_t within this interval and the corresponding residence time and selectivity for each scenario are shown in Fig. 9b. Obviously, the tube diameter does not have a significant impact on the selectivity. However, the residence time increases linearly with increasing tube diameter.

Based on the sensitivity analysis, it suffices to say that the selected constant heat transfer coefficient ($h = 0.5$ kW/(m^2 K)) will be sufficient for the technical approximation in level 3; while, the tube diameter will be kept as a decision variable because it influences the residence time.

4.3. Level 3: Technical approximation

In this section, we design an optimal technical reactor that approximates the control profiles derived in level 2. In the previous level, the environment temperature control was selected as the best control variable for the optimal reaction route of the S_NAr reaction. Based on Figs. 6–8, the heat flux of the best technical reactor can be approximated by first heating, maintaining the reaction temperature at the upper bound, and then cooling for the last 2.4 s. However, the time required for heating and cooling are relatively small when compared to the period of constant temperature. Hence, the technical reactor is further simplified by first using a pre-heater to heat the reactants to the maximum possible temperature; feeding the reactants into a tubular reactor that is maintained at the maximum temperature by a controller, and then using the controller to switch to cooling as soon as 99% conversion is achieved. Therefore, only the tubular reactor section will be modeled in detail and optimized in the following sections.

Furthermore, we assume that the best technical reactor for this reaction has plug flow characteristics as a majority of small scale reactors are assumed to have these characteristics. To identify the optimal configuration of the technical reactor, the governing equations are derived in the next step.

4.3.1. Model development for EPF level 3

Assuming no axial mixing, a constant reactor volume of 10 mL and an average fluid velocity, the continuous tubular coil reactor can be modeled as a one-dimensional plug-flow reactor with a heat exchanger. First, the component mole balances are given as:

$$\frac{dn_i}{dz} = \frac{V}{v}\sum_m^{N_{reac}} \nu_{i,m} \cdot r_m \quad \forall i \in N_{comp}, \tag{11}$$

where v is the mean fluid velocity. Furthermore, the energy balance for the reacting fluid inside the tubular reactor is given as:

$$v \cdot \left(\frac{\sum_i^{N_{comp}} n_i c_{p,i}}{V_{reac}} + \frac{\rho_{EtOH} \cdot c_{p,EtOH}}{Mwt_{EtOH}} \right) \frac{dT}{dz} = -\left(a \cdot j_q + \sum_m^{N_{reac}} r_m \cdot \Delta H_m \right) \tag{12}$$

In contrast to level 2, the environment temperature (cooling/heating temperature) is not considered as a control variable. Rather, a balance is done over the environment temperature T_e as shown below:

$$\frac{dT_e}{dz} = K_e \cdot j_q \tag{13}$$

where K_e is an aggregated cooling/heating fluid-dependent parameter that ranges from −1 to 1 m K/W (see Appendix D and Refs. [21,35]).

Furthermore, the reaction fluid velocity and flow regime is constrained by the Reynolds number:

$$Re = \frac{\rho_{EtOH} \cdot v \cdot d_t}{\mu_{EtOH}} \tag{14}$$

Other dimensionless numbers such as the Damköhler, Fourier, or Bodenstein number might be considered leading to more informed choices of the reactor types as suggested by Nagy et al. [23]. More details on the model formulation in level 3 can be found in Appendix D.

4.3.2. Optimization formulations for EPF Level 3

Besides the DAE model developed in Section 4.3.1, the volume constraint (Eq. (9)); and reasonable bounds on the Reynolds number Re, the parameter K_e and the mean fluid velocity v are also included in the optimization for level 3. The heat transfer coefficient was also kept at constant value of 0.5 kW/(m^2 K).

Based on the above specifications, the optimization formulation for level 3 is given as:

$$\min_{\{l, v, d_t, V_{EtOH}, n_{1,0}, \gamma\}} \tau$$

subject to

- Mole balances: Eq. (11)
- Energy balance: Eq. (12)
- Coolant energy balance: Eq. (13)
- Reaction rates: Eqs. (3) and (4)
- Performance measures: Eqs. (5) and (6)
- Volume constraint: Eq. (9)
- Reactor length: $l = 4 \cdot V/(\pi d_t^2)$
- Terminal constraint: $\mathcal{X} = 0.99$
- Heat loss constraint: $(T_f - T_0)^2 \leqslant 1$
- Intrinsic bounds: $T \in [T_L, T_U], T_e \in [T_{eL}, T_{eU}], \gamma \in [\gamma_L, \gamma_U]$
- Design bounds: $d_t \in [d_{tL}, d_{tU}], Re \in [Re_L, Re_U]$
- System bounds: $\mathcal{S} \in [0, 1]$

The optimization parameters and variable bounds used in level 3 are the same as those of level 2, with the exception of the lower and upper bound of the Reynolds number which were set at $Re_L = 100$ and $Re_U = 7000$, respectively. These bounds were chosen to keep the flow between the laminar and transition regimes. Note that the reactor length l is left as a free variable.

4.3.3. Results for level 3

The minimum residence time, selectivity, and optimal design variables for level 3 are summarized in Table 3. These results imply that the small-scale coil tubular reactor proposed in level 3 is able to technically approximate the optimal reaction route obtained in previous levels quite well. The residence time at level 3 is slightly longer than that of level 2 because of the introduction of more non-idealities. In order to determine possible materials that could be used to fabricate the reactor, a rough *back-of-the-envelope* calculation can be performed ($k \simeq h \times d_t \sim 0.70 W/(mK)$). Thus, a stainless steel material can be used for the optimal technical reactor [55].

Table 3
Optimal objective and design variables results for level 3.

Variable name	Values	Units
Residence time, τ (objective)	3.36	min
Selectivity, S	86	%
Feed ratio, γ	3:1	–
Heating fluid constant, K_e	0	m K/W
Internal tube diameter, d_t	1.42	mm
Reactor length, l	6.3	m
Fluid velocity, v	31.14	mm/s
Reynolds number, Re	7000	–

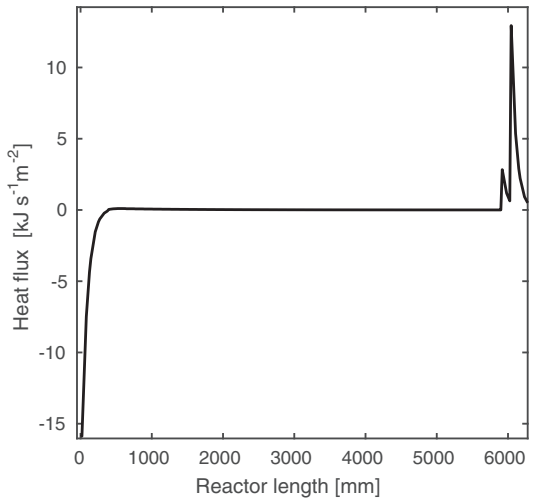

Fig. 10. Heat flux profile for the EPF level 3.

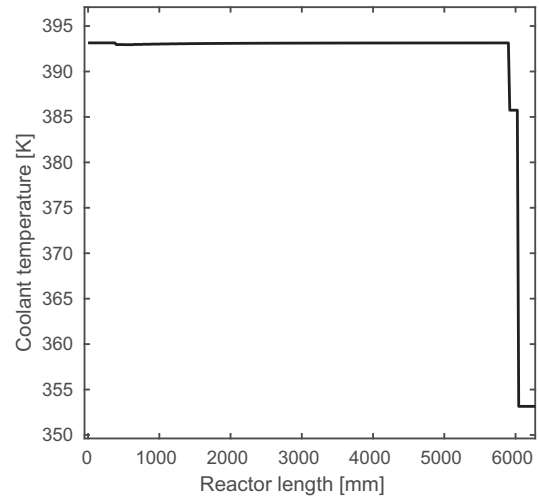

Fig. 12. Environment temperature control profile for the EPF level 3.

Moreover, the concentration profiles in level 3 are similar to those on level 2 and as such are not shown. The heat flux profile shows rapid heating from −15.88 to 0.099 kJ/(s m^2) until position 0.58 m in order to fulfill 99% conversion (see Fig. 10). Following this, the heat flux decreases gradually to 0.003 kJ/(s m^2) at position 5.90 m since the reaction now generates sufficient heat to sustain itself. At 5.90 m, 99% conversion is attained and then the heat flux switches to cooling mode.

As a result, the reaction and environment temperatures decrease after position 5.90 m as shown Figs. 11 and 12, respectively. This behavior is to ensure that the reaction still maintains the 99% conversion while minimizing the energy costs. Furthermore, cooling at the tail-end of the reactor could be important if a subsequent reactor or separation unit operates at a temperature lower than the maximum temperature (393.15 K) of the S_NAr reaction.

For the reaction system considered and the assumptions made in this work, the EPF outcome implies that a continuous tubular coil reactor with controlled heating is the best reactor type to minimize the residence time. Moreover, our results suggest that using this reactor configuration will lead to a 33% reduction in residence time in comparison to a literature reference case [22], while achieving a selectivity and conversion of 86% and 99%, respectively.

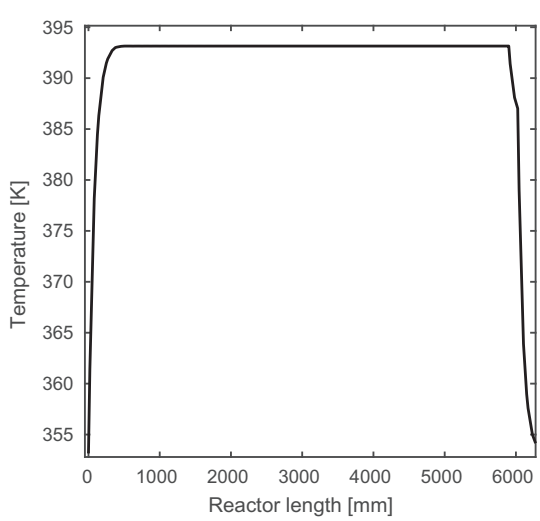

Fig. 11. Temperature state profile for the EPF level 3.

Please note that our predictions have not been experimentally verified, but are plausible in the context of the experiments conducted by Lee et al. [22]. Thus as part of a conceptual study, we have successfully demonstrated the principle use of the EPF concept in optimal reactor design for API synthesis problems.

5. Conclusions

In summary, we have demonstrated that the elementary process functions (EPF) approach can be used for the optimal design of reactors for API and organic intermediate production. As a model reaction, we considered the S_NAr reaction of 2,4-difluoronitrobenzene with morpholine and showed that the EPF approach leads to optimal design outcomes in terms of specified objective function.

The applicability of the EPF concept for any given process of interest is often hampered by the scarcity of available experimental data. To adapt the EPF approach to a particular API synthesis, the minimum required data are: a detailed reaction mechanism network, temperature-dependent reaction kinetic data, and the operating window in which the experiments were conducted.

In addition, information such as thermodynamic equilibrium data, physico-chemical properties of the reacting mixtures, fluid transport properties and a good engineering judgement will greatly improve the reliability of the results obtained by the EPF approach. Therefore, we conclude that the successful implementation of such an approach will require close collaboration and dialogue between process systems engineers and process chemists. Indeed, as the typical data provided by chemists or pharmaceutical researchers is insufficient for the EPF approach, additional reaction engineering experiments are required.

Nevertheless, unlike other simulation-based approaches and heuristics currently used in designing reactors for API synthesis, our approach inherits the apparatus-independent nature of the EPF concept. Even though the approach led to an existing reactor design in this case, it also has the advantage of leading to novel reactor designs [35,36].

In conclusion, applying the EPF approach for the design of reactors for API synthesis can lead to novel process windows [15]. Therefore, the approach can complement the experiments performed by process or organic chemists and speed-up the drug development process significantly.

Acknowledgement

We gratefully acknowledge the funding from the Ministry of Science and Culture, Lower Saxony, Germany under the SynFoBiA project– "Novel synthesis and formulation method for poorly soluble drugs and sensitive pharmaceuticals". The authors wish to thank Xiangzhong Xie and Moritz Schulze for their helpful comments on the initial manuscript. The authors also wish to thank Prof. Dr.-Ing. Andreas Seidel-Morgenstern and Dr. Ju Weon Lee for the fruitful discussion concerning their paper on the nucleophilic aromatic substitution of 2,4-difluoronitrobenzene. We also acknowledge Prof. Dr.-Ing. Kai Sundmacher and Nicolas Kaiser for the helpful discussions and assistance at the onset of this project.

Appendix A. Further results for level 1

For the second case in the first level (cf. Fig. A.13), reactant **1** starts at a concentration of 0.147 M and reacts instantaneously with **2** at time $t = 0$. As soon as the reaction begins, the remaining portion of **1** is dosed at 0.03 s with a molar flow rate of 16.29 mmol/min. This leads to a rapid increase of the concentration of **1** to 0.154 M followed by its gradual decrease along the reaction coordinate as it reacts with **2**. The residence time achieved by using the second concept results in a residence time of 3.22 min, and a selectivity of 86%.

Fig. A.14 shows the results for the third case, the results are quite similar to the results for the second case. However, reactant **2** is dosed instead of **1** in this case. Hence, the initial concentration **2** is 0.442 M but additional moles of **2** are dosed after 0.03 s with a molar flow rate of 48.94 mmol/min. The residence time and selectivity are also similar to that obtained in the second case.

Appendix B. Model assumptions for level 2

The specific heat capacity of the reacting species in Eq. (7) are expressed as polynomial functions of temperature. They are obtained by using least squares optimization in cases where experimental data from literature is available and by using group contributions in cases where they are not. Details of how the coefficients of the specific heat capacity equations are obtained are shown in C.

The left hand side of the energy balance equation above (cf. Eq. (7)), is made of contributions from the reacting species and the solvent (ethanol). The energy balance is formulated in such a way that only the specific heat capacities of the reacting species are dependent on temperature while the specific capacity of the solvent is assumed to vary negligibly with temperature. The assumption is valid for two reasons: (1) the model reaction considered is a homogeneous liquid phase reaction; (2) a rough *back-of-the-envelope* calculation reveals that the solvent occupies majority of the volume in the reference reactor. Moreover, this assumption reduces complexity of the model and intractable nonlinearities during subsequent optimization. The density of the solvent is also assumed to be constant since the reaction is a homogeneous liquid phase reaction.

Appendix C. Heat capacity

In this work, two approaches were used to obtain the specific heat capacity c_p equations. In the first approach, when specific heat capacity data are available in literature for a compound i, we assume that $c_{p,i}(T)$ follows a polynomial function of degree 2 as it provides a compromise between data fitting (see Figs. A.15 and A.16) and numerical robustness, i.e. avoiding overfitting and Runge's phenomenon:

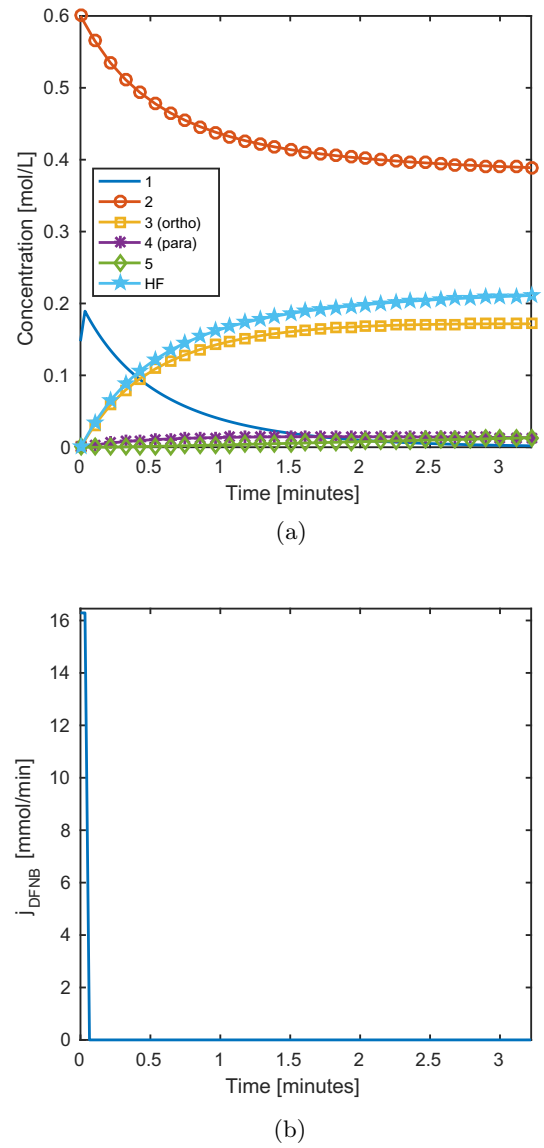

Fig. A.13. Optimization results for level 1, case 1 (τ = 3.22 min, γ = 3.00): (a) concentration state profiles; (b) dosing of **1** control profile.

$$c_{p,i}(T) = \alpha_i + \beta_i T + \gamma_i T^2 \tag{15}$$

and then we use least squares optimization[56] to estimate the coefficients α_i, β_i, and γ_i

$$\min \|\mathbf{A}_i \hat{\mathbf{x}}_i - \mathbf{b}_i\|_2 \tag{16}$$

where

$\mathbf{A}_i \hat{\mathbf{x}}_i - \mathbf{b}_i$ is the residual or error,

$\mathbf{b}_i = (c_{p,i,1}, c_{p,i,2}, \ldots, c_{p,i,k})$ is the specific heat capacities (outcomes) measured at different temperatures (observables) k,

$\hat{\mathbf{x}}_i = (\alpha_i, \beta_i, \gamma_i) \in \mathbb{R}^3$ is a vector containing the least-squares estimated coefficients for component i and,

$\mathbf{A}_i \in \mathbb{R}^{k \times N_{comp}}$ is a Vandermonde matrix with ($k \geqslant N_{comp}$).

$$\mathbf{A}_i = \begin{bmatrix} 1 & T_1 & T_1^2 \\ 1 & T_2 & T_2^2 \\ \vdots & \vdots & \vdots \\ 1 & T_k & T_k^2 \end{bmatrix} \tag{17}$$

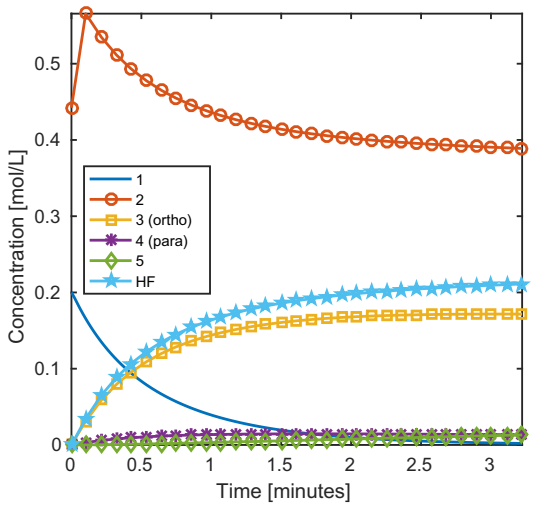

(a)

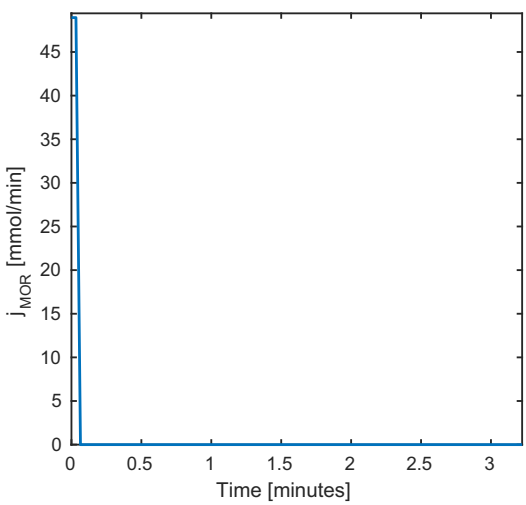

(b)

Fig. A.14. Optimization results for level 1, case 2 (τ = 3.22 min, γ = 3.00): (a) concentration state profiles; (b) dosing of **2** control profile.

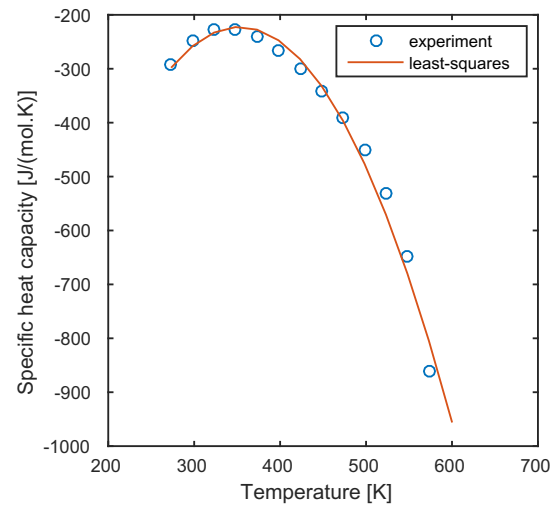

Fig. A.15. Determining the coefficients of the specific heat capacity equation for morpholine. The coefficients were determined by applying a second-order least square approximation on the experimental data from Mesmer and Hitch [57].

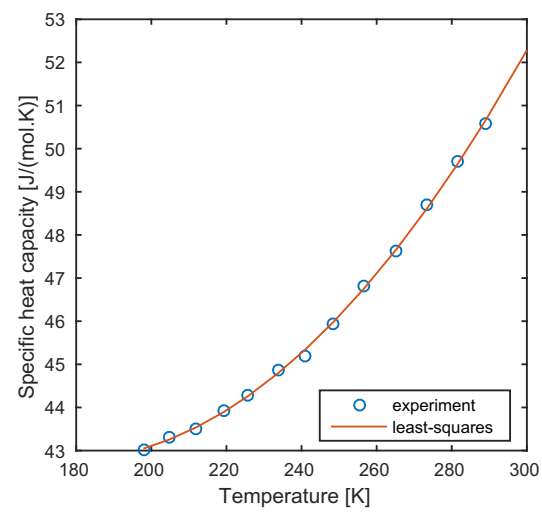

Fig. A.16. Determining the coefficients of the specific heat capacity equation for hydrogen fluoride. These coefficients were determined by applying a second-order least square approximation on experimental data [58].

The first approach was used to obtain the specific heat capacity equations for morpholine (**2**) [57] and hydrogen fluoride (HF) [58] (see Figs. A.16 and A.15).

For the other components for which specific heat capacity data could not be found, a group contribution method [59] given by the following equation was used:

$$c_{p,i}(T) = \sum_i n_i a_i + \sum_i n_i b_i T + \sum_i n_i c_i T^2 + \sum_i n_i d_i T^3 \tag{18}$$

where n_i is the number of occurrence of group i in a given molecule, a_i, b_i, c_i, and d_i are semi-empirical values associated with the group i, and T is the absolute temperature. Based on these two approaches, the coefficients for the specific heat equation for each compound are given in Table C.4.

Appendix D. Detailed model development for level 3

A detailed derivation of the coolant temperature T_e in level 3 reads as:

$$\frac{v_e \cdot \rho_e \cdot c_{p,e}}{\mathrm{Mwt}_e} \frac{dT_e}{dz} = \frac{\pi d_e}{A_e} \cdot j_q \tag{19}$$

K_e is an aggregated cooling fluid-dependent parameter that ranges from −1 to 1 min dm K/J [21,35] and it is given as:

$$K_e = \frac{\pi \cdot d_e \cdot \mathrm{Mwt}_e}{A_e \cdot v_e \cdot \rho_e \cdot c_{p,e}} \tag{20}$$

where Mwt_e is the molecular weight of the (cooling or heating) environment fluid, d_e is the diameter of the tube around the reactor in which the environment fluid flows, A_e is the cross-sectional area of the jacket around the reactor, v_e is the velocity of the environment fluid, ρ_e is the density of the environment fluid, and $c_{p,e}$ is the specific heat capacity of the environment fluid. These aforementioned parameters are assummed to be constant.

We also assume that the solvent occupies significant volume of the reactor. Based on this assumption, it suffices to assume that the Reynolds number will largely depend on the flow of the solvent (ethanol, EtOH).

Table C.4
Coefficients of specific heat capacity equations [22].

Species	α [J/(mol K)]	β [J/(mol K^2)]	γ [J/(mol K^3)]	δ [J/mol K^4]
1[a]	-1.912×10^1	5.700×10^{-1}	-3.761×10^{-4}	8.787×10^{-8}
2[b]	-1.712×10^{-3}	8.447×10^0	-1.198×10^{-2}	–
3[a]	-6.654×10^1	1.075×10^0	-7.132×10^{-4}	1.660×10^{-7}
4[b]	-6.654×10^1	1.075×10^0	-7.132×10^{-4}	1.660×10^{-7}
5[a]	-1.139×10^2	1.579×10^0	-1.050×10^{-3}	2.441×10^{-7}
HF[b]	6.251×10^1	-2.229×10^{-1}	6.294×10^{-4}	–
EtOH[c]	1.124×10^3	–	–	–

[a] Coefficients obtained from group contribution methods.
[b] Coefficients obtained from least-squares optimization.
[c] A constant value was used.

References

[1] D.M. Roberge, The complexity of technology implementation: flow versus batch processing, Chim. OGGI-Chem. Today 30 (2012) 5.
[2] D.M. Roberge, B. Zimmermann, F. Rainone, M. Gottsponer, M. Eyholzer, N. Kockmann, Microreactor technology and continuous processes in the fine chemical and pharmaceutical industry: is the revolution underway?, Org Process Res. Dev. 12 (5) (2008) 905–910, http://dx.doi.org/10.1021/op8001273.
[3] D. Roberge, Lonza–hazardous flow chemistry for streamlined large scale synthesis, Green Process. Synth. 1 (1) (2012) 129–130, http://dx.doi.org/10.1515/greenps-2011-0504.
[4] S.D. Schaber, D.I. Gerogiorgis, R. Ramachandran, J.M. Evans, P.I. Barton, B.L. Trout, Economic analysis of integrated continuous and batch pharmaceutical manufacturing: a case study, Ind. Eng. Chem. Res. 50 (17) (2011) 10083–10092, http://dx.doi.org/10.1021/ie2006752.
[5] H.G. Jolliffe, D.I. Gerogiorgis, Plantwide design and economic evaluation of two continuous pharmaceutical manufacturing (CPM) cases: ibuprofen and artemisinin, Comput. Chem. Eng. 91 (2016) 269–288, http://dx.doi.org/10.1016/j.compchemeng.2016.04.005.
[6] B. Gutmann, D. Cantillo, C.O. Kappe, Continuous-flow technology – a tool for the safe manufacturing of active pharmaceutical ingredients, Angew. Chem. Int. Ed. 54 (23) (2015) 6688–6728, http://dx.doi.org/10.1002/anie.201409318.
[7] D.I. Gerogiorgis, H.G. Jolliffe, Continuous pharmaceutical process engineering and economics, Chim. OGGI-Chem. Today 33 (2015) 6.
[8] R. Lakerveld, B. Benyahia, R.D. Braatz, P.I. Barton, Model-based design of a plant-wide control strategy for a continuous pharmaceutical plant, AIChE J. 59 (10) (2013) 3671–3685, http://dx.doi.org/10.1002/aic.14107.
[9] C. Jiménez-González, P. Poechlauer, Q.B. Broxterman, B.-S. Yang, D. am Ende, J. Baird, C. Bertsch, R.E. Hannah, P. DellÓrco, H. Noorman, Key green engineering research areas for sustainable manufacturing: a perspective from pharmaceutical and fine chemicals manufacturers, Org. Process Res. Dev. 15 (4) (2011) 900–911, http://dx.doi.org/10.1021/op100327d.
[10] C. Wiles, P. Watts, Improving chemical synthesis using flow reactors, Expert Opin. Drug Discov. 2 (11) (2007) 1487–1503, http://dx.doi.org/10.1517/17460441.2.11.1487.
[11] I.R. Baxendale, The integration of flow reactors into synthetic organic chemistry, J. Chem. Technol. Biotechnol. 88 (4) (2013) 519–552, http://dx.doi.org/10.1002/jctb.4012.
[12] A.R. Bogdan, S.L. Poe, D.C. Kubis, S.J. Broadwater, D.T. McQuade, The continuous-flow synthesis of ibuprofen, Angew. Chem. Int. Ed. 48 (45) (2009) 8547–8550, http://dx.doi.org/10.1002/anie.200903055.
[13] K. Gilmore, D. Kopetzki, J.W. Lee, Z. Horváth, D.T. McQuade, A. Seidel-Morgenstern, P.H. Seeberger, Continuous synthesis of artemisinin-derived medicines, Chem. Commun. 50 (84) (2014) 12652–12655, http://dx.doi.org/10.1039/C4CC05098C.
[14] D.R. Snead, T.F. Jamison, End-to-end continuous flow synthesis purification of diphenhydramine hydrochloride featuring atom economy, in-line separation, and flow of molten ammonium salts, Chem. Sci. 4 (7) (2013) 2822–2827, http://dx.doi.org/10.1039/C3SC50859E.
[15] V. Hessel, Novel process windows–gate to maximizing process intensification via flow chemistry, Chem. Eng. Technol. 32 (11) (2009) 1655–1681, http://dx.doi.org/10.1002/ceat.200900474.
[16] F.E. Valera, M. Quaranta, A. Moran, J. Blacker, A. Armstrong, J.T. Cabral, D.G. Blackmond, The flows the thing or is it? Assessing the merits of homogeneous reactions in flask and flow, Angew. Chem. Int. Ed. 49 (14) (2010) 2478–2485, http://dx.doi.org/10.1002/anie.200906095.
[17] P. Plouffe, A. Macchi, D.M. Roberge, From batch to continuous chemical synthesis – a toolbox approach, Org. Process Res. Dev. 18 (11) (2014) 1286–1294, http://dx.doi.org/10.1021/op5001918.
[18] D. Hildebrandt, D. Glasser, The attainable region and optimal reactor structures, Chem. Eng. Sci. 45 (8) (1990) 2161–2168, http://dx.doi.org/10.1016/0009-2509(90)80091-R.
[19] L. Achenie, L.T. Biegler, A superstructure based approach to chemical reactor network synthesis, Comput. Chem. Eng. 14 (1) (1990) 23–40, http://dx.doi.org/10.1016/0098-1354(90)87003-8.
[20] H. Freund, K. Sundmacher, Towards a methodology for the systematic analysis design of efficient chemical processes: Part 1. From unit operations to elementary process functions, Chem. Eng. Process. 47 (12) (2008) 2051–2060, http://dx.doi.org/10.1016/j.cep.2008.07.011.
[21] A. Peschel, H. Freund, K. Sundmacher, Methodology for the design of optimal chemical reactors based on the concept of elementary process functions, Ind. Eng. Chem. Res. 49 (21) (2010) 10535–10548, http://dx.doi.org/10.1021/ie100476q.
[22] J.W. Lee, Z. Horvath, A.G. O'Brien, P.H. Seeberger, A. Seidel-Morgenstern, Design and optimization of coupling a continuously operated reactor with simulated moving bed chromatography, Chem. Eng. J. 251 (2014) 355–370, http://dx.doi.org/10.1016/j.cej.2014.04.043.
[23] K.D. Nagy, B. Shen, T.F. Jamison, K.F. Jensen, Mixing and dispersion in small–scale flow systems, Org. Process Res. Dev. 16 (5) (2012) 976–981, http://dx.doi.org/10.1021/op200349f.
[24] P. Witt, S. Somasi, I. Khan, D. Blaylock, J. Newby, S. Ley, Modeling mesoscale reactors for the production of fine chemicals, Chem. Eng. J. 278 (2015) 353–362, http://dx.doi.org/10.1016/j.cej.2014.12.030.
[25] H.G. Jolliffe, D.I. Gerogiorgis, Process modelling and simulation for continuous pharmaceutical manufacturing of ibuprofen, Chem. Eng. Res. Des. 97 (2015) 175–191, http://dx.doi.org/10.1016/j.cherd.2014.12.005.
[26] C. Shukla, A. Kulkarni, V. Ranade, Selectivity engineering of the diazotization reaction in a continuous flow reactor, React. Chem. Eng. http://dx.doi.org/10.1039/C5RE00056D.
[27] H.G. Jolliffe, D.I. Gerogiorgis, Process modelling and simulation for continuous pharmaceutical manufacturing of artemisinin, Chem. Eng. Res. Des. 112 (2016) 310–325, http://dx.doi.org/10.1016/j.cherd.2016.02.017.
[28] T. Westermann, L. Mleczko, Heat management in microreactors for fast exothermic organic syntheses–first design principles, Org. Process Res. Dev. 20 (2) (2016) 487–494, http://dx.doi.org/10.1021/acs.oprd.5b00205.
[29] D.M. Roberge, What is flow chemistry?, Chim OGGI-Chem. Today 33 (2015) 4.
[30] P. Barthe, C. Guermeur, O. Lobet, M. Moreno, P. Woehl, D.M. Roberge, N. Bieler, B. Zimmermann, Continuous multi-injection reactor for multipurpose production – Part I, Chem. Eng. Technol. 31 (8) (2008) 1146–1154, http://dx.doi.org/10.1002/ceat.200800132.
[31] D.M. Roberge, N. Bieler, M. Mathier, M. Eyholzer, B. Zimmermann, P. Barthe, C. Guermeur, O. Lobet, M. Moreno, P. Woehl, Development of an industrial multi-injection microreactor for fast and exothermic reactions – Part II, Chem. Eng. Technol. 31 (8) (2008) 1155–1161, http://dx.doi.org/10.1002/ceat.200800131.
[32] P. Stonestreet, A. Harvey, A mixing-based design methodology for continuous oscillatory flow reactors, Chem. Eng. Res. Des. 80 (1) (2002) 31–44, http://dx.doi.org/10.1205/026387602753393204.
[33] D.L. Browne, B.J. Deadman, R. Ashe, I.R. Baxendale, S.V. Ley, Continuous flow processing of slurries: evaluation of an agitated cell reactor, Org. Process Res. Dev. 15 (3) (2011) 693–697, http://dx.doi.org/10.1021/op2000223.
[34] K.M. Christensen, M.J. Pedersen, K. Dam-Johansen, T.L. Holm, T. Skovby, S. Kiil, Design and operation of a filter reactor for continuous production of a selected pharmaceutical intermediate, Chem. Eng. Sci. 71 (2012) 111–117, http://dx.doi.org/10.1016/j.ces.2011.12.002.
[35] A. Peschel, F. Karst, H. Freund, K. Sundmacher, Analysis and optimal design of an ethylene oxide reactor, Chem. Eng. Sci. 66 (24) (2011) 6453–6469, http://dx.doi.org/10.1016/j.ces.2011.08.054.
[36] A. Peschel, B. Hentschel, H. Freund, K. Sundmacher, Design of optimal multiphase reactors exemplified on the hydroformylation of long chain alkenes, Chem. Eng. J. 188 (2012) 126–141, http://dx.doi.org/10.1016/j.cej.2012.01.123.
[37] A.I. Stankiewicz, J.A. Moulijn, et al., Process intensification: transforming chemical engineering, Chem. Eng. Prog. 96 (1) (2000) 22–34.
[38] R. Bakker, H. Van den Akker, A lagrangian description of micromixing in a stirred tank reactor using 1d-micromixing model in a CFD flow field, Chem. Eng. Sci. 51 (11) (1996) 2643–2648, http://dx.doi.org/10.1016/0009-2509(96)00130-3.
[39] L.T. Biegler, An overview of simultaneous strategies for dynamic optimization, Chem. Eng. Process. 46 (11) (2007) 1043–1053, http://dx.doi.org/10.1016/j.cep.2006.06.021.

[40] L.T. Biegler, Nonlinear Programming: Concepts, Algorithms, and Applications to Chemical Processes, vol. 10, SIAM, 2010.
[41] J.E. Cuthrell, L.T. Biegler, On the optimization of differential-algebraic process systems, AIChE J. 33 (8) (1987) 1257–1270.
[42] R. Fourer, D. Gay, B. Kernighan, AMPL. A Modelling Language for Mathematical Programming, second ed., Brooks/Cole Publishing Company, 2003.
[43] A.S. Drud, CONOPT – a large-scale GRG code, ORSA J. Comput. 6 (2) (1994) 207–216, http://dx.doi.org/10.1287/ijoc.6.2.207.
[44] A.G. O'Brien, Z. Horváth, F. Lévesque, J.W. Lee, A. Seidel-Morgenstern, P.H. Seeberger, Continuous synthesis and purification by direct coupling of a flow reactor with simulated moving-bed chromatography, Angew. Chem. Int. Ed. 51 (28) (2012) 7028–7030, http://dx.doi.org/10.1002/anie.201202795.
[45] B.J. Reizman, K.F. Jensen, An automated continuous-flow platform for the estimation of multistep reaction kinetics, Org. Process Res. Dev. 16 (11) (2012) 1770–1782, http://dx.doi.org/10.1021/op3001838.
[46] M. Charaschanya, A.R. Bogdan, Y. Wang, S.W. Djuric, Nucleophilic aromatic substitution of heterocycles using a high-temperature and high-pressure flow reactor, Tetrahedron Lett. 57 (9) (2016) 1035–1039, http://dx.doi.org/10.1016/j.tetlet.2016.01.080.
[47] H. Menard, R. Beaudoin, K. Loczy, Measurements of R0 (H) and R0 (F) in alcohol hydrogen fluoride mixtures, J. Chem. Eng. Data 29 (2) (1984) 120–121, http://dx.doi.org/10.1021/je00036a004.
[48] H.S. Fogler, Elements of Chemical Reaction Engineering, fourth ed., Prentice-Hall, 2006.
[49] J. Haber, B. Jiang, T. Maeder, N. Borhani, J. Thome, A. Renken, L. Kiwi-Minsker, Intensification of highly exothermic fast reaction by multi-injection microstructured reactor, Chem. Eng. Process. 84 (2014) 14–23, http://dx.doi.org/10.1016/j.cep.2014.02.007.
[50] B. Hentschel, A. Peschel, H. Freund, K. Sundmacher, Simultaneous design of the optimal reaction and process concept for multiphase systems, Chem. Eng. Sci. 115 (2014) 69–87, http://dx.doi.org/10.1016/j.ces.2013.09.046.
[51] A. ElSibai, L.K. RihkoStruckmann, K. Sundmacher, Model-based optimal Sabatier reactor design for power-to-gas applications, Energy Technol. http://dx.doi.org/10.1002/ente.201600600.
[52] Y. Lu, A.G. Dixon, W.R. Moser, Y.H. Ma, Analysis optimization of cross-flow reactors with staged feed policies–isothermal operation with parallel-series, irreversible reaction systems, Chem. Eng. Sci. 52 (8) (1997) 1349–1363, http://dx.doi.org/10.1016/S0009-2509(96)00491-5.
[53] C. Hamel, S. Thomas, K. Schädlich, A. Seidel-Morgenstern, Theoretical analysis of reactant dosing concepts to perform parallel-series reactions, Chem. Eng. Sci. 58 (19) (2003) 4483–4492, http://dx.doi.org/10.1016/S0009-2509(03)00308-7.
[54] N. Kockmann, M. Gottsponer, B. Zimmermann, D.M. Roberge, Enabling continuous-flow chemistry in microstructured devices for pharmaceutical and fine-chemical production, Chem. – A Eur. J. 14 (25) (2008) 7470–7477, http://dx.doi.org/10.1002/chem.200800707.
[55] H.P. Gemoets, Y. Su, M. Shang, V. Hessel, R. Luque, T. Noël, Liquid phase oxidation chemistry in continuous-flow microreactors, Chem. Soc. Rev. 45 (1) (2016) 83–117, http://dx.doi.org/10.1039/C5CS00447K.
[56] S. Boyd, L. Vandenberghe, Convex Optimization, Cambridge University Press, 2004.
[57] R. Mesmer, B. Hitch, Base strength of amines at high temperatures. Ionization of cyclohexylamine and morpholine, J. Solut. Chem. 6 (4) (1977) 251–261, http://dx.doi.org/10.1007/BF00645456.
[58] J.-H. Hu, D. White, H. Johnston, The heat capacity, heat of fusion and heat of vaporization of hydrogen fluoride, J. Am. Chem. Soc. 75 (5) (1953) 1232–1236, http://dx.doi.org/10.1021/ja01101a066.
[59] D. Rihani, L. Doraiswamy, Estimation of heat capacity of organic compounds from group contributions, Ind. Eng. Chem. Fundam. 4 (1) (1965) 17–21, http://dx.doi.org/10.1021/i160013a003.